A study on the ground state in interchain coupled quasi-one-dimensional organic

ferromagnets

A study on the ground state in interchain coupled quasi-one-dimensional organic ferromagnets

W Z Wang† and K L Yao‡

† Department of Physics, Huazhong University of Science and Technology, Wuhan 430074, People's Republic of China
‡ CCAST (World Laboratory), PO Box 8730, Beijing 100080, People's Republic of China, and International Centre of Material Physics, Academy Sinica, Shenyang 110015, People's Republic of China

Abstract. We deal with two neighbouring π-conjugated organic ferromagnetic chains with a Hamiltonian including the Hubbard on-site electron–electron repulsion and nearest-neighbouring Coulomb repulsion. We take into account the interchain coupling as an interchain electron-transfer term, which is different with respect to different sites in chains. The distribution of charge density, the ferromagnetic order and the stability of the high-spin ground state are studied in detail. It is shown that the nearest-neighbouring Coulomb repulsion leads to inhomogeneous distribution of charge density and spin density with respect to different sites. The interchain coupling results in transfers of charge density and spin density between the main chain and the side radicals. The interchain coupling stabilizes the high-spin ground state while the nearest-neighbouring Coulomb repulsion makes it unstable.

1. Introduction

In recent years, with the discovery of organic conductors and organic superconductors, there is much interest in the design of organic ferromagnets. Several research groups in the world have successfully synthesized several organic ferromagnets from organic molecules and hydrocarbons, such as m-PDPC [1] and p-NPNN [2]. The search for organic ferromagnets has attracted considerable attention [3–7]. However, most efforts are focused on the experimental exploration for improving ferromagnetism of these materials. The mechanism of ferromagnetism in these organic ferromagnets has not been established clearly.

McConnell [8] first proposed to produce intermolecular ferromagnetic interactions in organic molecules in 1963. Nasu [9] investigated a quasi-one-dimensional (quasi-1D) organic ferromagnet called m-PDPC using a periodic Kondo–Hubbard model. Ovchinnikov and Spector [10] developed a simplified model (a single chain in figure 1) to describe the ferromagnetic ordering in organic materials. The main chain consists of carbon atoms each with a π electron and R is a kind of side radical containing an unpaired electron. They treated the π electrons along the main chain as an antiferromagnetic spin chain, and assumed that there exists antiferromagnetic correlation between the π-electron spin and the residual spin of the side radical. Considering the strong electron–electron interaction, the electron–phonon coupling and the antiferromagnetic correlation between itinerant π electrons and the localized unpaired electrons at side radicals, Fang *et al* [11, 12] have proposed a theoretical model for the quasi-1D organic ferromagnet and obtained a ferromagnetic ground state, in
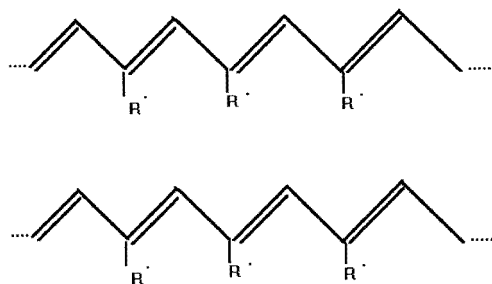
Figure 1. Two neighbouring chains of a quasi-1D organic ferromagnet.

which a parallel spin arrangement of the unpaired electrons at the side free radical can be gained and there exists an antiferromagnetic spin density wave along the main chain. Fang *et al* [13] also discussed the situation in which the unpaired electrons at side radicals can hop between the main chain and the side radicals. They obtained a ferromagnetic ground state with high spin. Adding the nearest-neighbouring electron–electron repulsion to the Hamiltonian, they obtained a redistribution of charge density and spin density [14]. However, in their works, the system was treated as an isolated chain. Although most organic polymers have a linear chain structure with weak interchain coupling, in some situations interchain coupling can have a significant effect as will be proved in this paper. Thus, first, we will propose a theoretical model including the nearest-neighbouring Coulomb repulsion and the interchain interaction to deal with the interchain coupled quasi-1D organic ferromagnet. Based on the topological structure of the system, the interchain coupling is considered as interchain electron transfer and is different with respect to different sites in the chain. In section 2, we will give the theoretical model and the computational method. Results and discussion will be given in section 3.

2. The model Hamiltonian and the numerical method

We consider two neighbouring coupled chains shown in figure 1. Based on the discussion in section 1, the Hamiltonian employed in our study can be written as

$$H = H_0 + H' \tag{1}$$

where H_0 is the Hamiltonian of two isolated chains without interchain coupling and H' describes the interchain coupling. We can write H_0 explicitly as follows:

$$H_0 = H_1 + H_2 \tag{2}$$

$$H_1 = -\sum_{jl\sigma}[t_0 + \gamma(u_{jl} - u_{jl+1})](c_{j1l\sigma}^+ c_{j1l+1\sigma} + \text{HC}) - \sum_{jl\sigma}(T_1 c_{j1l\sigma}^+ c_{j2l\sigma}\delta_l + \text{HC})$$

$$+\frac{\kappa}{2}\sum_{jl}(u_{jl} - u_{jl+1})^2 \tag{3}$$

$$H_2 = U\sum_{jl}(n_{j1l\alpha}n_{j1l\beta} + n_{j2l\alpha}n_{j2l\beta}\delta_l) + V\sum_{jl\sigma\sigma'}(n_{j1l\sigma}n_{j1l+1\sigma'} + n_{j1l\sigma}n_{j2l\sigma'}\delta_l). \tag{4}$$

The first term H_1 describes the intrachain hoppings of the π electrons on each main chain and unpaired electrons at side radicals, the electron–phonon interaction and the distortion of the lattice, where $c_{jil\sigma}^+$ ($c_{jil\sigma}$) denotes the creation (annihilation) operator of a π electron ($i = 1$) along each main chain or an unpaired electron ($i = 2$) at a side radical with spin

σ on the lth site in the jth chain, t_0 is the hopping integral of the π electron along each main chain when there is no dimerization, T_1 is the hopping integral between a π electron on the main chain and an unpaired electron at the side radical, γ is the electron–phonon coupling constant, u_{jl} is the displacement of the lth site on the jth main chain and κ is the elastic constant of the lattice. We assume that the side radicals connect with the even carbon atoms; then

$$\begin{aligned} \delta_l &= 1 \qquad l \text{ is even} \\ \delta_l &= 0 \qquad l \text{ is odd.} \end{aligned} \tag{5}$$

H_2 describes the Hubbard on-site electron–electron repulsion (the first term in H_2) and the nearest-neighbouring Coulomb repulsion (the second term in H_2) of π electrons and unpaired electrons at side radicals. $n_{jil\sigma} = c_{jil\sigma}^+ c_{jil\sigma}$ ($\sigma = \alpha, \beta$) where α and β denote up spin and down spin respectively.

Considering the topological structure of the system, we assume the interchain coupling in the following form:

$$H' = -\sum_{l\sigma}[T_2(1-\delta_l) + T_3\delta_l](c_{11l\sigma}^+ c_{21l\sigma} + \text{HC}) - T_4\sum_{l\sigma}(c_{12l\sigma}^+ c_{22l\sigma}\delta_l + \text{HC}) \tag{6}$$

where T_2 (T_3) are interchain electron transfers from the odd site (even site) in the first chain to the corresponding odd site (even site) and T_4 is the interchain hopping integral from the side radical in the first chain to the corresponding side radical in the second one.

It is convenient to cast all quantities into dimensionless forms as

$$h = \frac{H}{t_0} \qquad u = \frac{U}{t_0} \qquad v = \frac{V}{t_0} \qquad t_i = \frac{T_i}{t_0} \qquad (i = 1, 2, 3, 4) \tag{7}$$

$$\lambda = \frac{2\gamma^2}{t_0\pi\kappa} \qquad y_{jl} = (-1)^l(u_{jl} - u_{jl+1})\gamma/t_0.$$

So the Hamiltonian h becomes

$$h = h_e + h' \tag{8}$$

$$\begin{aligned} h_e = &-\sum_{jl\sigma}[1 + (-1)^l y_{jl}](c_{j1l\sigma}^+ c_{j1l+1\sigma} + \text{HC}) - \sum_{jl\sigma}(t_1 c_{j1l\sigma}^+ c_{j2l\sigma}\delta_l + \text{HC}) \\ &+ u\sum_{jl}(n_{j1l\alpha}n_{j1l\beta} + n_{j2l\alpha}n_{j2l\beta}\delta_l) + v\sum_{jl\sigma\sigma'}(n_{j1l\sigma}n_{j1l+1\sigma'} + n_{j1l\sigma}n_{j2l\sigma'}\delta_l) \\ &-\sum_{l\sigma}(t_4 c_{12l\sigma}^+ c_{22l\sigma}\delta_l + \text{HC}) - \sum_{l\sigma}[t_2(1-\delta_l) + t_3\delta_l](c_{11l\sigma}^+ c_{21l\sigma} + \text{HC}) \end{aligned} \tag{9}$$

$$h' = \frac{1}{\pi\lambda}\sum_{jl}y_{jl}^2 \tag{10}$$

where h_e is the electronic part of the Hamiltonian and h' describes the elastic energy of the lattice.

Since we use the tight-binding approximation in the Hamiltonian (1), the wave function of the system can be expanded in site basis functions in the Wannier representation:

$$\Psi_\mu = \sum_{jil\sigma}Z_{\mu jil}^\sigma c_{jil\sigma}^+ |0\rangle \tag{11}$$

where $|0\rangle$ is the true electron vacuum state, Ψ_μ denotes the μth eigenvector of the Hamiltonian and $Z_{\mu jil}^\sigma$ is the expansion coefficient.

We can numerically solve the Schrödinger equation,

$$h_e\Psi_\mu = \varepsilon_\mu\Psi_\mu. \tag{12}$$

Here, ε_μ is the μth eigenvalue of (12). In the mean-field approximation we divide $n_{jil\sigma}$ as follows:

$$n_{jil\sigma} = \langle n_{jil\sigma} \rangle + \Delta n_{jil\sigma}$$
$$n_{jil\sigma} n_{j'i'l'\sigma'} = n_{jil\sigma} \langle n_{j'i'l'\sigma'} \rangle + n_{j'i'l'\sigma'} \langle n_{jil\sigma} \rangle - \langle n_{jil\sigma} \rangle \langle n_{j'i'l'\sigma'} \rangle \tag{13}$$

where $\langle \cdots \rangle = \langle G | \cdots | G \rangle$ is the average with respect to the ground state $|G\rangle$ and $\Delta n_{jil\sigma}$ is the fluctuation from the average value. In order to solve the equation (12) conveniently, we take the terms $\langle n_{jil\sigma} \rangle \langle n_{j'i'l'\sigma'} \rangle$ in (9) as constants and do not affect the configuration of the energy band.

From (9)–(13), we can write the eigenvalue equation explicitly after omitting the constant $\langle n_{jil\sigma} \rangle \langle n_{j'i'l'\sigma'} \rangle$:

$$\langle 0 | c_{j'i'l'\sigma'} h_e \sum_{jil\sigma} Z_{\mu jil}^\sigma c_{jil\sigma}^+ | 0 \rangle = \varepsilon_\mu^\sigma \langle 0 | c_{j'i'l'\sigma'} \sum_{jil\sigma} Z_{\mu jil}^\sigma c_{jil\sigma}^+ | 0 \rangle \tag{14}$$

namely

$$-[1+(-1)^l y_{1l}]Z_{\mu 11l+1}^\sigma - [1+(-1)^{l-1} y_{1l-1}]Z_{\mu 11l-1}^\sigma - t_1 \delta_l Z_{\mu 12l}^\sigma$$
$$+v \sum_{\substack{\sigma' \\ (occ)}} (\langle n_{11l+1\sigma'} \rangle + \langle n_{11l-1\sigma'} \rangle + \langle n_{12l\sigma'} \rangle \delta_l) Z_{\mu 11l}^\sigma + u \langle n_{11l\bar\sigma} \rangle Z_{\mu 11l}^\sigma$$
$$-[t_2(1-\delta_l) + t_3 \delta_l] Z_{\mu 21l}^\sigma = \varepsilon_\mu^\sigma Z_{\mu 11l}^\sigma \tag{15}$$

$$\left(u \langle n_{12l\bar\sigma} \rangle Z_{\mu 12l}^\sigma - t_1 Z_{\mu 11l}^\sigma - t_4 Z_{\mu 22l}^\sigma + v \sum_{\substack{\sigma' \\ (occ)}} \langle n_{11l\sigma'} \rangle Z_{\mu 12l}^\sigma \right) \delta_l = \varepsilon_\mu^\sigma Z_{\mu 12l}^\sigma \tag{16}$$

$$-[1+(-1)^l y_{2l}]Z_{\mu 21l+1}^\sigma - [1+(-1)^{l-1} y_{2l-1}]Z_{\mu 21l-1}^\sigma - t_1 \delta_l Z_{\mu 22l}^\sigma$$
$$+v \sum_{\substack{\sigma' \\ (occ)}} (\langle n_{21l+1\sigma'} \rangle + \langle n_{21l-1\sigma'} \rangle + \langle n_{22l\sigma'} \rangle \delta_l) Z_{\mu 21l}^\sigma + u \langle n_{21l\bar\sigma} \rangle Z_{\mu 21l}^\sigma$$
$$-[t_2(1-\delta_l) + t_3 \delta_l] Z_{\mu 11l}^\sigma = \varepsilon_\mu^\sigma Z_{\mu 21l}^\sigma \tag{17}$$

$$\left(u \langle n_{22l\bar\sigma} \rangle Z_{\mu 22l}^\sigma - t_1 Z_{\mu 21l}^\sigma - t_4 Z_{\mu 12l}^\sigma + v \sum_{\substack{\sigma' \\ (occ)}} \langle n_{21l\sigma'} \rangle Z_{\mu 22l}^\sigma \right) \delta_l = \varepsilon_\mu^\sigma Z_{\mu 22l}^\sigma. \tag{18}$$

Here, $\bar\sigma = \alpha \delta_{\beta\sigma} + \beta \delta_{\alpha\sigma}$.

The total energy of the system with the Hamiltonian (8) is:

$$E(\{y_{jl}\}) = -\sum_{jl\sigma}[1+(-1)^l y_{jl}] \sum_{\substack{\mu \\ (occ)}} (Z_{\mu j1l+1}^{\sigma*} Z_{\mu j1l}^\sigma + Z_{\mu j1l}^{\sigma*} Z_{\mu j1l+1}^\sigma)$$
$$+\frac{1}{\pi\lambda} \sum_{jl} y_{jl}^2 - t_1 \sum_{jl\sigma} \sum_{\substack{\mu \\ (occ)}} (Z_{\mu j1l}^{\sigma*} Z_{\mu j2l}^\sigma + Z_{\mu j2l}^{\sigma*} Z_{\mu j1l}^\sigma) \delta_l$$
$$-\sum_{l\sigma} t_4 \sum_{\substack{\mu \\ (occ)}} (Z_{\mu 12l}^{\sigma*} Z_{\mu 22l}^\sigma + Z_{\mu 22l}^{\sigma*} Z_{\mu 12l}^\sigma)$$
$$-\sum_{l\sigma}[t_2(1-\delta_l) + t_3 \delta_l] \sum_{\substack{\mu \\ (occ)}} (Z_{\mu 11l}^{\sigma*} Z_{\mu 21l}^\sigma + Z_{\mu 21l}^{\sigma*} Z_{\mu 11l}^\sigma)$$
$$+u \sum_{jl} \left(\sum_{\substack{\mu\mu' \\ (occ)}} |Z_{\mu j1l}^\alpha|^2 |Z_{\mu' j1l}^\beta|^2 + \sum_{\substack{\mu\mu' \\ (occ)}} |Z_{\mu j2l}^\alpha|^2 |Z_{\mu' j2l}^\beta|^2 \delta_l \right)$$
$$+v \sum_{jl} \left[\sum_{\substack{\mu\mu'\sigma\sigma' \\ (occ)}} |Z_{\mu j1l}^\sigma|^2 |Z_{\mu' j1l}^{\sigma'}|^2 + \sum_{\substack{\mu\mu'\sigma\sigma' \\ (occ)}} |Z_{\mu j1l}^\sigma|^2 |Z_{\mu' j2l}^{\sigma'}|^2 \delta_l \right]. \tag{19}$$

The dimerization y_{jl} can be obtained by minimizing the total energy of the system with respect to y_{jl}:

$$y_{jl} = \pi\lambda(-1)^l\left[\sum_{\substack{\mu\sigma \\ (occ)}} Z^\sigma_{\mu j1l}Z^\sigma_{\mu j1l+1} - \frac{1}{N}\sum_l\sum_{\substack{\mu\sigma \\ (occ)}} Z^\sigma_{\mu j1l}Z^\sigma_{\mu j1l+1}\right]. \tag{20}$$

Here, we have used the periodic boundary condition; N is the number of sites along each main chain. For two chains, (14)–(18) have $6N$ energy eigenvalues but there are only $2N\,\pi$ electrons along the main chain and N unpaired electrons at the side radicals, so the energy bands are half filled. In order to discuss the ground state, we fill the electrons in those states with lowest energy, which are labelled with (occ) in (14)–(20). The distribution of spin density δn_{jil} and charge density $\langle n_{jil}\rangle$ of π electrons and unpaired electron at side radicals can be obtained self-consistently as

$$\delta n_{jil} = \frac{1}{2}(\langle n_{jil\alpha}\rangle - \langle n_{jil\beta}\rangle) = \frac{1}{2}\sum_{\substack{\mu \\ (occ)}}(|Z^\alpha_{\mu jil}|^2 - |Z^\beta_{\mu jil}|^2) \tag{21a}$$

$$\langle n_{jil}\rangle = \langle n_{jil\alpha}\rangle + \langle n_{jil\beta}\rangle = \sum_{\substack{\mu\sigma \\ (occ)}}|Z^\sigma_{\mu jil}|^2. \tag{21b}$$
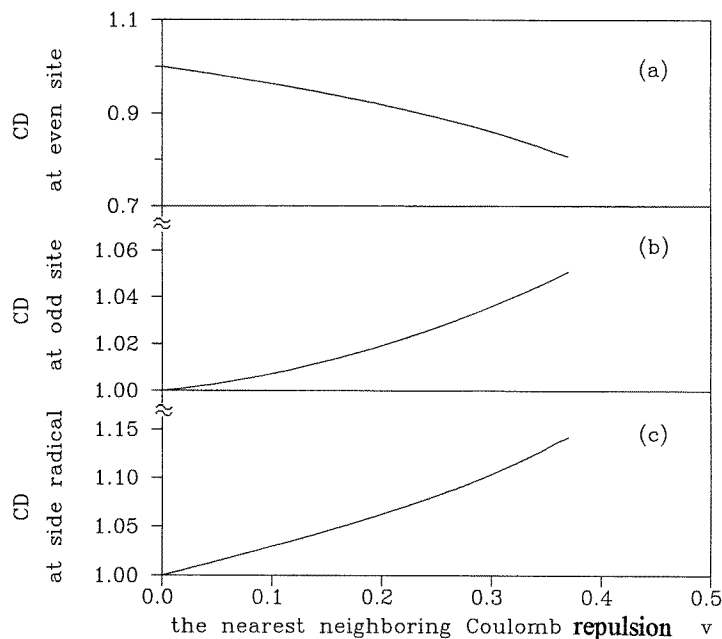

Figure 2. The charge density at different sites versus the nearest-neighbouring Coulomb repulsion v: (a) at the even sites on each main chain; (b) at the odd sites on each main chain; (c) at the side radicals for $t_2 = t_3 = t_4 = 0.1$.

The energy eigenvalue ε^σ_μ and the expansion coefficients $Z^\sigma_{\mu jil}$ can be obtained from (14)–(21) self-consistently. The starting geometry in the iterative optimization process is usually the one with $y_{jl} = 0$ and $\langle n_{jil\alpha}\rangle = \langle n_{jil\beta}\rangle = \frac{1}{2}$. The starting geometry in the
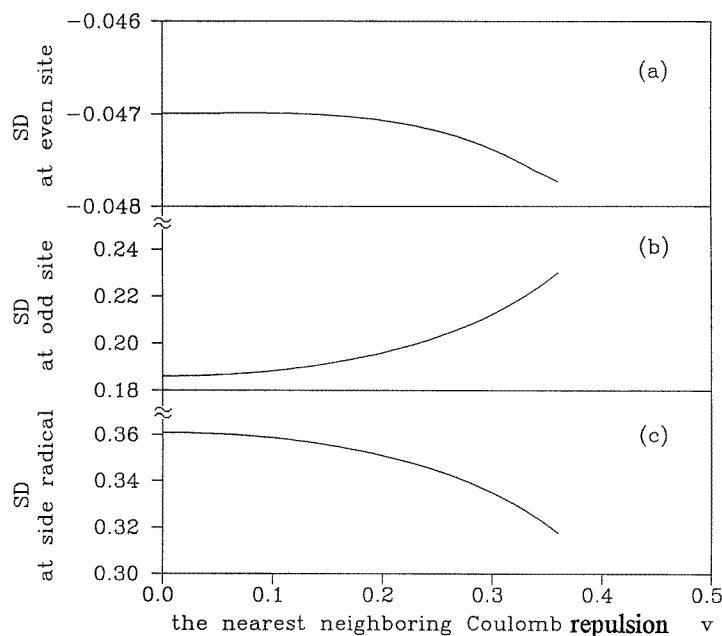
Figure 3. The spin density at different sites versus the nearest-neighbouring Coulomb repulsion v: (a) at the even sites on each main chain; (b) at the odd sites on each main chain; (c) at the side radicals for $t_2 = t_3 = t_4 = 0.1$.

iterative optimization process is usually the one with zero dimerization. The stability of the optimized geometry is always tested by using another starting configuration and performing the optimization once again. A set of solutions are reached, independent of the starting configuration. The criterion for terminating the optimization is that between two successive iterations, the differences are less than 10^{-7} for the dimerization and spin density.

3. Results and discussion

Figure 1 shows the structure considered in this paper. Each organic chain contains 40 π electrons each on the carbon atoms and 20 unpaired electrons each on the side radicals connecting with the even carbon atoms. Apparently, the eigenvalue equations (14)–(18) are unsymmetrical about spin owing to the extended Hubbard electron–electron repulsion term. We must solve the eigenvalue equations with different spins. In order to study the ground state, we always fill the π electrons and unpaired electrons at the side radicals in the possible lowest levels in every iterative step. In the following discussions, we assume the parameters $\lambda = 0.4$, $u = 1.0$ and $t_1 = 0.9$. We will discuss the effect of the nearest-neighbouring Coulomb repulsion and interchain coupling on the charge density, spin density and stability of the ferromagnetic ground state of the system.

For the π-conjugated organic chain shown in figure 1, considering the Hubbard on-site repulsion and itineracy of π electrons along the main chain and the unpaired electron at the side radicals, Fang *et al* [13] have obtained a high-spin ground state in which the ferromagnetism is mainly contributed by the side radicals and charge density is distributed
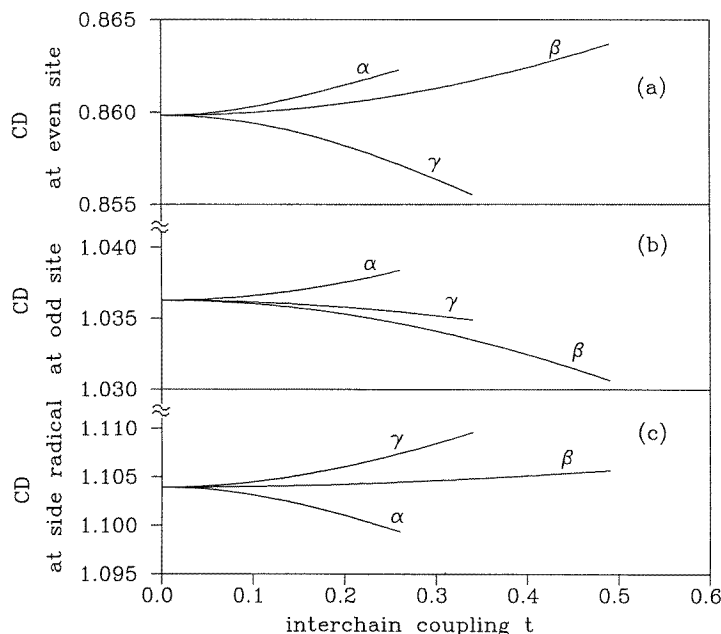
Figure 4. The charge density at different sites against the interchain coupling t for $v = 0.3$: (a) at the even sites on each main chain; (b) at the odd sites on each main chain; (c) at the side radicals. Curve α is for $t = t_2$, $t_3 = t_4 = 0$, curve β for $t = t_3$, $t_2 = t_4 = 0$ and curve γ for $t = t_4$, $t_2 = t_3 = 0$.

uniformly on the main chain and side radicals. However, when we consider the interchain coupling and the nearest-neighbouring Coulomb repulsion, the charge density and spin density will be redistributed inhomogeneously at side radicals and along the main chain. In figures 2 and 3, we take the interchain coupling $t_2 = t_3 = t_4 = 0.1$. Figure 2 shows the charge density (CD) along the main chain and on the side radicals versus the nearest-neighbouring repulsion v. We find that with increasing nearest-neighbour Coulomb repulsion v, the charge density at even sites decreases while the charge density at odd sites and side radicals increases. This means that the nearest-neighbouring repulsion makes the electrons transfer from even sites to odd sides and side radicals. Comparing figure 2(b) with (c), we can see that the electrons on even sites mainly transfer to side radicals. This result can be understood since the radical is a free radical which is only subjected to the repulsive interaction of the connected even site while each site along the main chain is contemporaneously subjected to the Coulomb repulsion of the sites to its right and left. The charge density slightly transfers from even sites to odd sites because the electrons on even sites are subjected to the repulsions of the nearest odd sites and the connected side radicals while the electrons on odd sites are only subjected to the repulsion of the nearest even sites. Figure 3 shows the spin density (SD) versus the nearest-neighbouring Coulomb repulsion v. In the calculation, we take up spin as positive and down spin as negative. From figure 3, we can see that the ground state of the system is still a high-spin state since the sum of spins is a large positive value. It is shown that with increasing v the spin density at the odd site increases, while the spin densities at the even site and the side radical decrease. Moreover, the sum of the spin of the main chain increases while the sum of the spins of
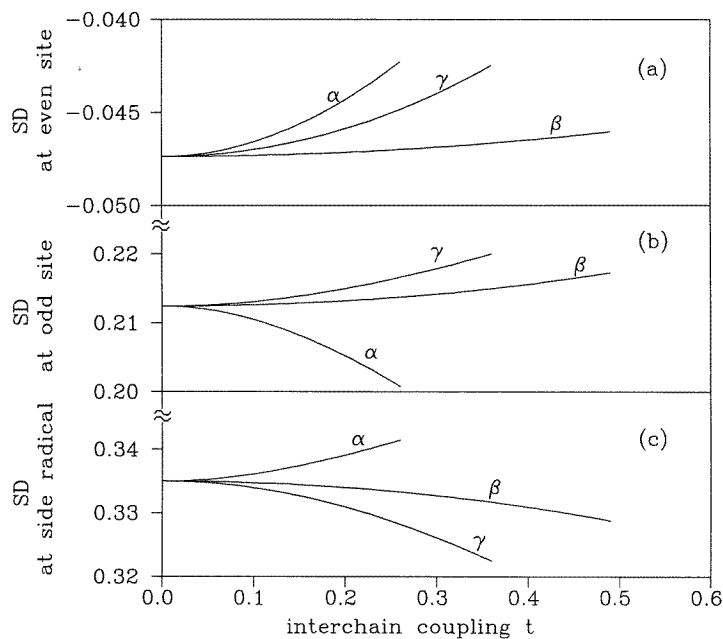
Figure 5. The spin density at different sites against the interchain coupling t for $v = 0.3$: (a) at the even sites on each main chain; (b) at the odd sites on each main chain; (c) at the side radicals. Curve α is for $t = t_2$, $t_3 = t_4 = 0$, curve β for $t = t_3$, $t_2 = t_4 = 0$ and curve γ for $t = t_4$, $t_2 = t_3 = 0$.

the side radicals decreases. This means that, with increasing v, the contribution of the main chain to the ferromagnetism of the system increases and that of the side radical decreases. Comparing figure 2(c) and figure 3(c), we find that, with increasing v, it is mainly down-spin electrons that transfer to the side radicals from the even sites. Comparing figure 2(b) and figure 3(b), we find that it is mainly up-spin electrons that transfer to the odd sites. We also find that the total energy of the system increases with increasing nearest-neighbouring Coulomb repulsion v, so the nearest-neighbouring Coulomb repulsion makes the high-spin ground state unstable.

Then, we discuss the effect of the interchain coupling on the high-spin ground state. In figures 4–6, we assume the nearest-neighbouring Coulomb repulsion $v = 0.3$. For curves α, β and γ, the interchain coupling corresponds to the following: $t = t_2$, $t_3 = t_4 = 0$; $t = t_3$, $t_2 = t_4 = 0$ and $t = t_4$, $t_3 = t_2 = 0$, respectively. Figure 4 shows the charge density at different sites as a function of interchain coupling t. From curves α in figure 4(a)–(c), we find that the interchain hopping t_2 between the corresponding odd sites of two neighbouring chains makes the electrons transfer from the side radicals to the main chain. Curves β in figure 4 show that with increasing interchain coupling t_3 between the even sites the charge density transfers from the odd sites to the even sites and side radicals. Curves γ in figure 4 show that as the interchain hopping t_4 between side radicals increases the charge density transfers from the main chain to the side radicals. Figure 5 shows the spin density at different sites as a function of interchain coupling t. From curves α in figure 5, we can see that with increasing t_2 the spin density transfers from the odd site to the even sites and side radicals. Comparing curves α in figure 4 with curves α in figure 5, we find that it is
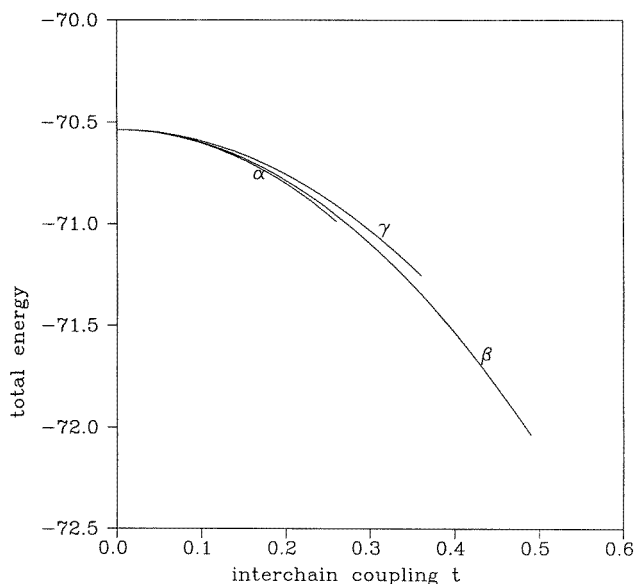
Figure 6. The total energy of the system against the interchain coupling t for $v = 0.3$. Curve α is for $t = t_2$, $t_3 = t_4 = 0$, curve β for $t = t_3$, $t_2 = t_4 = 0$ and curve γ for $t = t_4$, $t_2 = t_3 = 0$.

mainly down-spin electrons that transfer from the side radicals to the main chain. Curves β in figure 5 show that the interchain coupling t_3 enables the spin density to transfer from the side radicals to the main chain. Comparing curves β with γ in figure 5, we find that the interchain coupling t_3 and t_4 has a similar effect on the transfer of spin density, but the effect of t_4 is greater than that of t_3. Figure 6 shows that the total energy of the system varies with the interchain coupling t. It is shown that increasing interchain coupling makes the total energy decrease. This means that the interchain coupling stabilizes the high-spin ground state.

To sum up, we have studied a theoretical model for an interchain coupled quasi-1D organic ferromagnet. It is shown that the nearest-neighbouring Coulomb repulsion leads to inhomogeneous distribution of charge density and spin density. Different interchain couplings result in different transfers of charge density and spin density. The interchain coupling stabilizes the high-spin ground state while the electron–electron repulsion between the nearest-neighbouring sites makes the ground state unstable.

Acknowledgment

References

[1] Iwamura H, Sugawra T, Itoh K and Takui T 1985 *Mol. Cryst. Liq. Cryst.* **125** 379
[2] Takahashi M, Turek P, Nakazawa Y, Tamura M, Nozawa K, Shioni D, Ishikawa M and Kinoshita M 1991 *Phys. Rev. Lett.* **67** 746
[3] Bagus P S and Torrance J B 1989 *Phys. Rev.* B **9** 7301
[4] Macedo A M S, dos Santos M C, Coutinho-Filho M D and Macedo C A 1995 *Phys. Rev. Lett.* **74** 1851

  [5] Kawamoto T, Shirai M and Suzuki N 1995 *Synth. Met.* **71** 1789
  [6] Tanaka K, Ago H and Yamabe T 1995 *Synth. Met.* **72** 225
  [7] Koneravka M, Kellnerova V, Kopcansky P and Kuczynski T 1995 *J. Magn. Magn. Mater.* **140–144** 1455
  [8] McConnell H M 1963 *J. Chem. Phys.* **39** 1901
  [9] Nasu K 1986 *Phys. Rev.* B **33** 330
 [10] Ovchinnikov A A and Spector V N 1988 *Synth. Met.* **27** B615
 [11] Fang Z, Liu Z L and Yao K L 1994 *Phys. Rev.* B **49** 3916
 [12] Fang Z, Liu Z L and Yao K L 1995 *Phys. Rev.* B **51** 1304
 [13] Fang Z, Liu Z L and Yao K L 1995 *40th Conf. on Magnetism and Magnetic Materials (Philadelphia, PA, 1995)*
 [14] Fang Z, Liu Z L and Yao K L 1995 *J. Phys. C: Solid State Phys.* **7** 8429